

Benefits of Linear Conditioning for Segmentation using Metadata

Andreeanne Lemay^{1,2}

ANDREANNE.LEMAY@POLYMTL.CA

¹ *NeuroPoly Lab, Institute of Biomedical Engineering, Polytechnique Montreal, Canada*

² *Mila, Quebec AI Institute, Canada*

Charley Gros^{1,2}

CHARLEY.GROS@GMAIL.COM

Olivier Vincent^{1,2}

OVINCENT.POLY@GMAIL.COM

Yaou Liu³

YAOULIU80@163.COM

³ *Beijing Tiantan Hospital, Capital Medical University, China*

Joseph Paul Cohen^{*2,4}

JOSEPH@JOSEPHPCOHEN.COM

⁴ *Stanford University Center for Artificial Intelligence in Medicine & Imaging*

Julien Cohen-Adad^{*1,2,5}

JCOHEN@POLYMTL.CA

⁵ *Functional Neuroimaging Unit, CRIUGM, University of Montreal, Montreal, Canada*

Editors: Under Review for MIDL 2021

Abstract

Medical images are often accompanied by metadata describing the image (vendor, acquisition parameters) and the patient (disease type or severity, demographics, genomics). This metadata is usually disregarded by image segmentation methods. In this work, we adapt a linear conditioning method called FiLM (**F**eature-**w**ise **L**inear **M**odulation) for image segmentation tasks. This FiLM adaptation enables integrating metadata into segmentation models for better performance. We observed an average Dice score increase of 5.1% on spinal cord tumor segmentation when incorporating the tumor type with FiLM. The metadata modulates the segmentation process through low-cost affine transformations applied on feature maps which can be included in any neural network’s architecture. Additionally, we assess the relevance of segmentation FiLM layers for tackling common challenges in medical imaging: training with limited or unbalanced number of annotated data, multi-class training with missing segmentations, and model adaptation to multiple tasks. Our results demonstrated the following benefits of FiLM for segmentation: FiLMed U-Net was robust to missing labels and reached higher Dice scores with few labels (up to 16.7%) compared to single-task U-Net. The code is open-source and available at www.ivadomed.org.

Keywords: Deep learning, linear conditioning, segmentation, metadata, task adaptation.

1. Introduction

Segmentation tasks in the medical domain are often associated with metadata: medical condition of the patients, demographic specifications, acquisition center, acquisition parameters, etc. Depending on which structure is segmented, these metadata can help deep learning models improve their performance, however, metadata is usually overlooked. In this work, we improve segmentation models using recent advances in visual question answering called FiLM (Perez et al., 2018; de Vries et al., 2017) (**F**eature-**w**ise **L**inear **M**odulation). Using FiLM to condition a segmentation model enables the integration of prior metadata

* Contributed equally

into neural networks through linear modulation layers. The layer-specific affine coefficients are learned during training, enabling the model to modulate the segmentation output based on the input image and metadata. The metadata could also be exploited for task adaptation. When training a multi-class segmentation model, each class needs to be segmented on each image, as missing labels will hamper the learning (Zhou et al., 2019).

Label availability and quantity often represent a bottleneck in deep learning (Minaee et al., 2020). Segmentation is costly in terms of time, money, and logistics (Bhalgat et al., 2018). For instance, chest CT scans contain hundreds of 2D scans (up to 861 axial slices in the dataset used for this work) depending on the resolution. As reference, Google sets the price of image segmentation to 870 USD for 1000 images¹, which totals 435 USD for a single subject with 500 axial slices. For medical image segmentation requiring expert knowledge (e.g. tumor segmentation), this price could be higher considering the hourly wage of a radiologist. As for the time, (Ciga and Martel, 2021) reports that it takes between 15 minutes and two hours depending on the size and resolution to segment a single image of lymph nodes for breast cancer. An approach dealing with missing modalities and requiring less labels can reduce the monetary and time-related costs.

We hypothesize that conditioning the model based on the organ to be segmented (e.g., “kidney”, “liver”) will make it robust to missing segmentations. A multi-class model could then be trained on data from multiple datasets with a single class annotated in each. Since the different tasks share weights, fewer labels are required for a given class as the model can learn from the other tasks. This enables the model to easily adapt a single segmentation model to several tasks requiring only a small amount of annotations for novel tasks.

1.1. Prior work

Conditional linear modulation was introduced in many deep learning fields: visual reasoning (Perez et al., 2018; de Vries et al., 2017), style transfer (Dumoulin et al., 2017), speech recognition (Kim et al., 2017), domain adaptation (Li et al., 2018), few-shot learning (Oreshkin et al., 2018), to name a few. Feature-specific multiplicative and additive factors modulate the network to improve its performance.

The adaptation of FiLM (i.e., linear conditioning) for segmentation was first experimented on multiple sclerosis lesions with a FiLMed U-Net modulating the model with the modality exclusively (T2-weighted or T2star-weighted) (Vincent et al., 2020). Results were inconclusive regarding the performance of FiLM compared to a regular U-Net. A possible explanation for this lack of improvement is that the modality-related features might already be encoded in the regular U-Net, therefore the metadata added to FiLM is not informative enough, and thus does not translate to an increase in segmentation performance. In light of these results, in the present work we generalized the modified-FiLM implementation to be able to modulate a model by inputting any type of discrete metadata data.

1.2. Contribution

The key contributions of this work are:

(i) We introduce an adaptation of linear conditioning (Perez et al., 2018) based on metadata for segmentation tasks using the U-Net architecture.

1. <https://cloud.google.com/ai-platform/data-labeling/pricing>

(ii) We demonstrate that including metadata can contribute to the model’s performance. As a proof of concept, we input the spinal cord tumor type (astrocytoma, ependymoma, hemangioblastoma) which is often associated with its size, composition, and anatomical location. This resulted in a Dice score improvement of 5.1% over models trained without metadata.

(iii) We illustrate that linear modulation enables task adaptation with fewer labeled data when jointly trained on multiple tasks. A Dice score improvement of up to 16.7% was observed using our approach when training with a restricted number samples to simulate low data situations. Moreover, robust learning with missing modalities was achieved with FiLM.

2. Methods

2.1. Architecture and Implementation

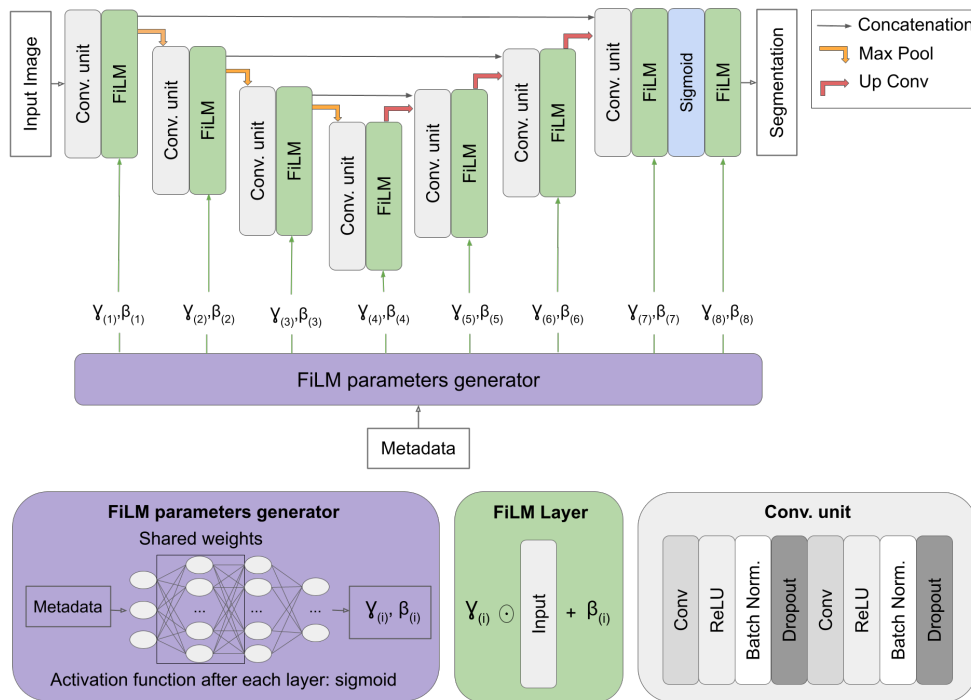


Figure 1: FiLMed U-Net architecture of depth 3. Depth describes the number of maximum pooling or up convolutions in the U-Net. γ and β values are generated using a multi-layer perceptron with shared weights across FiLM layers. γ and β have the same shape as the input. An element-wise multiplication is applied between the input and γ while the β is added. Conv.: convolutional; Norm.: normalization.

The core architecture is based on the 2D U-Net (Ronneberger et al., 2015) (Figure 1). The model has two inputs: the image and the one-hot encoded metadata (i.e., prior knowledge). FiLM layers and generator are responsible to condition the neural network with the given metadata. Two parameters, $\gamma_{(i)}$ and $\beta_{(i)}$, are required to linearly modulate the

inputs of the i^{th} FiLM layer. The metadata is passed through a multi-layer perceptron (i.e., FiLM generator) with two hidden layers (64 and 16 neurons). The FiLM generator outputs one value of γ and β for each filter (i.e., feature extractor) which are respectively multiplied and added by the FiLM layers to each convolutional feature map. The computational cost of FiLM is low and independent of the image resolution. The weights from the generator are shared for a more efficient learning (Perez et al., 2018). Since the input of the FiLM generator is the same, the same features should be extracted from the metadata. The values are constrained between 0 and 1 due to the sigmoid activation. Preliminary experiments favored sigmoid over ReLU or tanh activation function for the FiLM parameters. $\gamma_{(i)}$ values near 0 silence some features, while $\gamma_{(i)}$ values near 1 output the key features. Since the linear modulation is computationally inexpensive, FiLM layers were placed after each convolutional unit to ensure the metadata is properly used by the network. The code is open-source and available in the ivadomed toolbox (Gros et al., 2021).

2.2. Experiment 1: Segmentation using relevant metadata

The aim of this experiment was to assess the relevance of including prior metadata during the training.

2.2.1. DATASET: SPINAL CORD TUMOR

We used a spinal cord tumor segmentation dataset (Lemay et al., 2021). The dataset included 343 MRI scans, where each image was associated with one of the following tumor types: astrocytoma (101), ependymoma (122), or hemangioblastoma (120). The tumor type can be informative for the model since each type has particular characteristics, e.g., size, location, contrast intensity patterns, tissue constitution, (Kim et al., 2014; Baleriaux, 1999). Two modalities, Gadolinium-enhanced T1-weighted (Gd-e T1w) and T2-weighted (T2w), are required to properly segment each component of the tumor: tumor core, edema, and liquid-filled cavity. Here, for simplicity, only the tumor core labels were used.

2.2.2. TRAINING SCHEME

The first scenario used the FiLM architecture without any input metadata, while the second scenario included the tumor type as metadata. The same architecture was used in both scenarios in order to isolate the specific effect of the input metadata. Preliminary experiments gave similar results when using a regular U-Net architecture without the FiLM layers or a FiLMed U-Net with always the same input. A 320x256 sagittal image of resolution 1mmx1mm associated with the tumor type constituted one training sample. The dataset was split per patient with the following proportions: 60% training, 20% validation, 20% testing. To compare the overall segmentation performance, 10-fold cross-validations were performed.

2.3. Experiment 2: FiLM for multiple tasks

Here, the ability of FiLM to modulate the network to adapt to different segmentation tasks was assessed. The FiLMed model was presented with labels from three classes that are all present in the scan, but only one segmentation is presented. The class of the segmentation

presented to the network was input into the network to teach the model to properly segment each class. A similar experiment was performed with few segmentations and unbalanced datasets.

2.3.1. DATASET: SPLEEN, KIDNEYS, AND LIVER

The organs selected for this task were the spleen, kidneys, and liver. The datasets were collected from two different sources: Medical Segmentation Decathlon (Simpson et al., 2019) for spleen and liver scans, and KiTS19 (Heller et al., 2019) for kidney scans. Liver and kidney scans had tumor labeling which was ignored for the current experiments: organ and tumor annotations were merged as a single segmentation. Due to the large size of the kidney and liver datasets, subdatasets were extracted. Since the spleen dataset contained 41 scans with associated ground truths, only the first 41 kidney and liver scans were retained.

2.3.2. TRAINING SCHEME

First, the FiLMed U-Net was trained on the spleen, kidney, and liver images with the whole dataset (41 images for each). A training example was a 2D axial slice of 512x512 pixels paired with the available label (kidney, spleen, or liver). The dataset was split per patient with the following proportions: 60% training, 20% validation, 20% testing.

Second, to assess the performance on small datasets, FiLMed U-Net was trained on subdatasets of the spleen and kidney datasets. For simplicity, only two classes were used. The subdatasets were randomly chosen with a size of 2, 4, 6, 8, and 12 for one class and 12 subjects of the other class (i.e., total of 10 models: {2, 4, 6, 8, 12} spleens with 12 kidneys each and {2, 4, 6, 8, 12} kidneys with 12 spleens each). The size of the dataset included all the subjects for training and validation. The models were tested on 25 subjects of the class with the least subject. For a model trained on 2 kidney subjects and 12 spleen subjects, the model would be tested on 25 spleen subjects not included in the training or validation set. During the training process, the data was sampled to expose each class evenly to the model even when the number of subjects is unbalanced. All the trainings were repeated with a 10-fold cross-validations (100 trainings).

Regular 2D U-Nets trained on only one class at the time, spleen, kidney, or liver were trained following the same training, validation, and test splits for comparison.

2.4. Training parameters

The tumor types or organ labels were evenly separated in the three training, validation, and testing groups and the data were sampled with a batch size of 8. The FiLMed U-Nets of depth 4 for the spinal cord tumor and 5 for the chest CT were trained with a Dice loss function until the validation loss plateaued for 50 epochs (early stopping with $\epsilon = 0.001$). The depth was chosen according to the size of the input images. The initial learning rate was 0.001 and was modulated according to a cosine annealing learning rate.

2.5. Evaluation

The Dice score was selected to compare the performance of each approach. All FiLMed approaches were compared with the conventional approach: training without informative

metadata for spinal cord tumor and on a regular U-Net for the multi-organ segmentation tasks. To assess the statistical differences between group, a one-sided Wilcoxon signed-rank test with a p-value $< 5\%$ was considered to be a significant difference.

3. Results

3.1. Experiment 1: Segmentation using relevant metadata

Prior knowledge of the tumor type led to a significant Dice score improvement between the regular U-Net and the FiLMed U-Net: 10.5% for the hemangioblastomas (p-value=0.006), 4.5% for the astrocytomas (p-value=0.003), and 5.1% for all tumors combined (p-value=0.003) (Table 1). Astrocytomas and hemangioblastomas showed the highest Dice score gain when the model was informed with the tumor type. Astrocytomas are typically large, have ill-defined boundaries, and present heterogeneous, moderate, or partial enhanced in the Gd-e T1w contrast (Baleriaux, 1999). Conversely, hemangioblastomas are usually associated with a small tumor core (Baleriaux, 1999) intensely enhanced on Gd-e T1w (Baker et al., 2000). These distinctive characteristics can be learned by the model to perform a more informed segmentation (see Appendix to visualize segmentation differences).

Table 1: Spinal cord tumor core segmentation performance for regular and FiLMed U-Net (mean \pm STD % for 10 cross-validations). The FiLMed U-Net was trained with the tumor type as input. ** p-value < 0.05 for one-sided Wilcoxon signed-rank test.

Tumor type	Dice score [%]	
	No prior info.	Prior info.
Hemangioblastoma	51.2 \pm 4.0	61.7 \pm 3.7 **
Ependymoma	57.2 \pm 3.2	57.7 \pm 2.4
Astrocytoma	53.3 \pm 4.8	57.8 \pm 4.9 **
All	54.0 \pm 2.2	59.1 \pm 2.3 **

3.2. Experiment 2: FiLM for multiple tasks

Table 2 shows that the FiLMed multi-class model trained on 41 subjects of each class (i.e., kidney, spleen, and liver) was able to reach equivalent performance (i.e., no statistical difference) to single-class U-Nets. For reference, the Dice scores reached by other authors on the healthy tissue of organs from the whole challenge datasets, 61 spleens, 300 kidneys, and 201 livers, with 2D U-Nets was included. Even with subdatasets (i.e., 41 images per dataset), our 2D U-Nets reached Dice scores near the ones from other works.

Figure 2 demonstrates the ability of FiLMed U-Net to be trained on small or unbalanced datasets. With the same amount of labels for a given class, FiLMed models reached superior Dice scores for datasets of size 2, 4, 6, and 8 compared with the regular U-Nets trained on a single class, 11.5%, 16.7%, 5.5%, and 4.7%, respectively. This suggests that the FiLMed models were able to learn from the images associated with the other task. For instance, with only 2 kidney and 12 spleen labels the FiLMed model was associated with higher Dice scores for kidney segmentation compared with a regular U-Net trained with 2 kidney

Table 2: Multiple-organ segmentation with FiLMed and regular U-Nets (mean \pm STD %). The FiLMed U-Net was trained on spleen, kidney, and liver while regular U-Nets were trained on each class independently. A one-sided Wilcoxon signed-rank test was performed on the Dice scores of the two first columns. No statistical difference were observed between FiLM and regular trainings.

Task	Our experiments		Literature
	2D U-Net (1 model/task)	FiLMed 2D U-Net (1 model for all tasks)	2D U-Net (On whole challenge dataset)
Liver	95.1 \pm 1.4	94.1 \pm 1.6	95.3 \pm N/A (Isensee et al., 2019)
Spleen	91.7 \pm 6.3	92.2 \pm 5.3	94.2 \pm N/A (Isensee et al., 2019)
Kidney	90.4 \pm 9.3	90.7 \pm 8.1	93.0 \pm 1.2 (Ahmed, 2020)

segmentations, while also being able to annotate spleens. The more subjects are included in the dataset, the more the performances are similar for FiLMed vs. regular U-Net. However, FiLMed models have the advantage to segment more than one class without the need to label all classes in the image unlike the regular approach. The addition of FiLM layers to the regular U-Net achieved similar performances than regular model trained on each target independently, but only one model was needed to achieve this multi-target task, instead of three models. Even with unbalance between the number of segmentations (e.g., 2 spleen and 12 kidney labels), the FiLMed model was able to outperform the single-class U-Net.

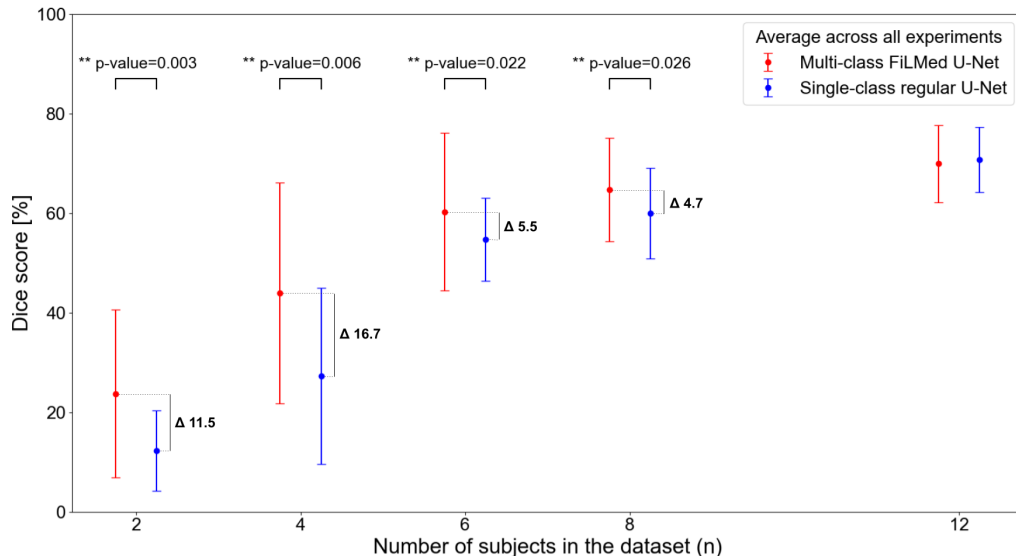


Figure 2: Spleen and kidney segmentation Dice scores for small and unbalanced datasets. The number of subjects combine training and validation subjects. Dice scores for all experiments on the test set (25 subjects) were averaged across the number of subjects and aggregated according to the approach, FiLMed U-Net (red) or regular U-Net (blue). The error bars show the standard deviation. Δ indicates the difference of mean Dice scores between the two approaches. The data totals 10 cross-validations. ** p-value < 5% with one-sided Wilcoxon signed-rank test.

4. Discussion

FiLM provides a flexible, low computational cost option to integrate prior knowledge. In this paper, the type of spinal cord tumor was exploited as a proof of concept, but the possibilities of metadata that can improve the performance of a model are vast. The prior metadata could include domain information (e.g., acquisition center, scanner vendor), anatomical data (e.g., location in the body, pose estimation, disease type or severity), or rater specification (e.g., rater’s experience, rater’s id). To elaborate on an example, inter-expert variability is an important aspect in medical segmentation (Renard et al., 2020). Integrating this information in the model would enable one to make predictions according to the rater with the most experience or to create a model that can replicate inter-expert predictions (i.e., generating one prediction per expert learned in training).

FiLM is capable of dealing with missing segmentation labels by indicating which annotations are presented to the model. With the rise of artificial intelligence, there are more and more datasets available online. However, the majority include segmentation for only one or two classes. FiLM makes it possible to use data from different sources with only one class annotated to create a multi-class model, instead of single-class models trained on each dataset. Without the need for more annotations, combining datasets increases the number of examples seen by the model. Since weights are shared between tasks, the model learns from the data of the other tasks as seen in Figure 2. The transfer learning between tasks and the robustness with respect to missing segmentations reduce the number of annotations required.

Since the metadata is one-hot encoded before being introduced in the FiLM generator, discrete prior information is needed. The approach presented works with continuous data (e.g., age, size, MRI acquisition parameters), but it must be discretized into a binned range. Future work should focus on adapting the method to input continuous values. This enhancement would allow the integration of MRI acquisition parameters (e.g., echo-time, flip angle) that might make the model agnostic to the different acquisition sequences.

5. Conclusion

The integration of linear conditioning through FiLM for segmentation models enables a flexible option to integrate metadata to enhance the predictions. FiLM also facilitates the training of multi-class models by being robust to missing labels and requiring less data than a conventional single class U-Net on small datasets. Future work could focus on the impact of integrating other type of data than the tumor type, increasing the number of tasks performed by a single FiLMed model, or evaluating the impact of including prior information on the model’s uncertainty.

Acknowledgments

We thank the contributors of the ivadomed repository, Lucas Rouhier, Ainsleigh Hill, Valentine Louis-Lucas, and Christian Perone for fruitful discussion.

Funded by the Canada Research Chair in Quantitative Magnetic Resonance Imaging [950-230815], the Canadian Institute of Health Research [CIHR FDN-143263], the Canada Foundation for Innovation [32454, 34824], the Fonds de Recherche du Québec - Santé

[28826], the Fonds de Recherche du Québec - Nature et Technologies [2015-PR-182754], the Natural Sciences and Engineering Research Council of Canada [RGPIN-2019-07244], the Canada First Research Excellence Fund (IVADO and TransMedTech), the Courtois NeuroMod project and the Quebec BioImaging Network. A.L. has a fellowship from NSERC, FRQNT and UNIQUE, C.G. has a fellowship from IVADO [EX-2018-4], O.V. has a fellowship from NSERC, FRQNT and UNIQUE.

References

- Mohamed Ahmed. Medical image segmentation using attention-based deep neural networks, 2020. URL <https://www.diva-portal.org/smash/get/diva2:1477227/FULLTEXT01.pdf>.
- Kim B Baker, Christopher J Moran, Franz J Wippold, James G Smirniotopoulos, Fabio J Rodriguez, Steven P Meyers, and Todd L Siegal. Mr imaging of spinal hemangioblastoma. *American Journal of Roentgenology*, 174(2):377–382, 2000. URL <https://www.ajronline.org/doi/full/10.2214/ajr.174.2.1740377>.
- DLF Baleriaux. Spinal cord tumors. *European radiology*, 9(7):1252–1258, 1999. URL <https://doi.org/10.1007/s003300050831>.
- Yash Bhalgat, Meet Shah, and Suyash Awate. Annotation-cost minimization for medical image segmentation using suggestive mixed supervision fully convolutional networks. In *Neural Information Processing Systems (NeurIPS)*, 2018. URL <https://arxiv.org/pdf/1812.11302.pdf>.
- Ozan Ciga and Anne L Martel. Learning to segment images with classification labels. *Medical Image Analysis*, 68:101912, 2021. URL <https://doi.org/10.1016/j.media.2020.101912>.
- Harm de Vries, Florian Strub, Jérémie Mary, Hugo Larochelle, Olivier Pietquin, and Aaron C. Courville. Modulating early visual processing by language. In *Neural Information Processing Systems (NIPS)*, pages 6597–6607, 2017. URL <http://papers.nips.cc/paper/7237-modulating-early-visual-processing-by-language>.
- Vincent Dumoulin, Jonathon Shlens, and Manjunath Kudlur. A learned representation for artistic style. In *International Conference on Learning Representations (ICLR)*, 2017. URL <https://arxiv.org/pdf/1610.07629.pdf>.
- Charley Gros, Andreanne Lemay, Olivier Vincent, Lucas Rouhier, Marie-Helene Bourget, Anthime Bucquet, Joseph Paul Cohen, and Julien Cohen-Adad. ivadomed: A medical imaging deep learning toolbox. *Journal of Open Source Software*, 6(58):2868, 2021. URL <https://doi.org/10.21105/joss.02868>.
- Nicholas Heller, Niranjan Sathianathen, Arveen Kalapara, Edward Walczak, Keenan Moore, Heather Kaluzniak, Joel Rosenberg, Paul Blake, Zachary Rengel, Makinna Oestreich, et al. The kits19 challenge data: 300 kidney tumor cases with clinical context, ct semantic segmentations, and surgical outcomes. *arXiv preprint arXiv:1904.00445*, 2019. URL <https://arxiv.org/pdf/1904.00445.pdf>.

- Fabian Isensee, Paul F Jäger, Simon AA Kohl, Jens Petersen, and Klaus H Maier-Hein. Automated design of deep learning methods for biomedical image segmentation. *arXiv preprint arXiv:1904.08128*, 2019. URL <https://arxiv.org/pdf/1904.08128.pdf>.
- DH Kim, J-H Kim, Seung Hong Choi, C-H Sohn, Tae Jin Yun, Chi Heon Kim, and K-H Chang. Differentiation between intramedullary spinal ependymoma and astrocytoma: comparative mri analysis. *Clinical radiology*, 69(1):29–35, 2014. URL <https://doi.org/10.1016/j.crad.2013.07.017>.
- Taesup Kim, Inchul Song, and Yoshua Bengio. Dynamic layer normalization for adaptive neural acoustic modeling in speech recognition. In *InterSpeech*, 2017. URL <https://arxiv.org/pdf/1707.06065.pdf>.
- Andreean Lemay, Charley Gros, Zhizheng Zhuo, Jie Zhang, Yunyun Duan, Julien Cohen-Adad, and Yaou Liu. Multiclass spinal cord tumor segmentation on mri with deep learning, 2021. URL <https://arxiv.org/pdf/2012.12820.pdf>.
- Yanghao Li, Naiyan Wang, Jianping Shi, Xiaodi Hou, and Jiaying Liu. Adaptive batch normalization for practical domain adaptation. *Pattern Recognition*, 80:109–117, 2018. URL <https://doi.org/10.1016/j.patcog.2018.03.005>.
- Shervin Minaee, Yuri Boykov, Fatih Porikli, Antonio Plaza, Nasser Kehtarnavaz, and Demetri Terzopoulos. Image segmentation using deep learning: A survey. *arXiv preprint arXiv:2001.05566*, 2020. URL <https://arxiv.org/pdf/2001.05566.pdf>.
- Boris N Oreshkin, Pau Rodriguez, and Alexandre Lacoste. Tadam: Task dependent adaptive metric for improved few-shot learning. *arXiv preprint arXiv:1805.10123*, 2018. URL <https://arxiv.org/pdf/1805.10123.pdf>.
- Ethan Perez, Florian Strub, Harm De Vries, Vincent Dumoulin, and Aaron Courville. Film: Visual reasoning with a general conditioning layer. In *Proceedings of the AAAI Conference on Artificial Intelligence*, volume 32, 2018. URL <https://arxiv.org/pdf/1709.07871.pdf>.
- Félix Renard, Soulaïmane Guedria, Noel De Palma, and Nicolas Vuillerme. Variability and reproducibility in deep learning for medical image segmentation. *Scientific Reports*, 10(1):1–16, 2020. URL <https://doi.org/10.1038/s41598-020-69920-0>.
- Olaf Ronneberger, Philipp Fischer, and Thomas Brox. U-net: Convolutional networks for biomedical image segmentation. In *Medical Image Computing and Computer-Assisted Intervention – MICCAI 2015*, pages 234–241. Springer International Publishing, 2015. URL https://doi.org/10.1007/978-3-319-24574-4_28.
- Amber L Simpson, Michela Antonelli, Spyridon Bakas, Michel Bilello, Keyvan Farahani, Bram Van Ginneken, Annette Kopp-Schneider, Bennett A Landman, Geert Litjens, Björn Menze, et al. A large annotated medical image dataset for the development and evaluation of segmentation algorithms. *arXiv preprint arXiv:1902.09063*, 2019. URL <https://arxiv.org/pdf/1902.09063.pdf>.

Olivier Vincent, Charley Gros, Joseph Paul Cohen, and Julien Cohen-Adad. Automatic segmentation of spinal multiple sclerosis lesions: How to generalize across mri contrasts?, 2020. URL <https://arxiv.org/pdf/2003.04377.pdf>.

Yuyin Zhou, Zhe Li, Song Bai, Chong Wang, Xinlei Chen, Mei Han, Elliot Fishman, and Alan L Yuille. Prior-aware neural network for partially-supervised multi-organ segmentation. In *Proceedings of the IEEE/CVF International Conference on Computer Vision*, pages 10672–10681, 2019. URL <https://arxiv.org/pdf/1904.06346.pdf>.

Appendix A. Spinal cord tumor segmentation

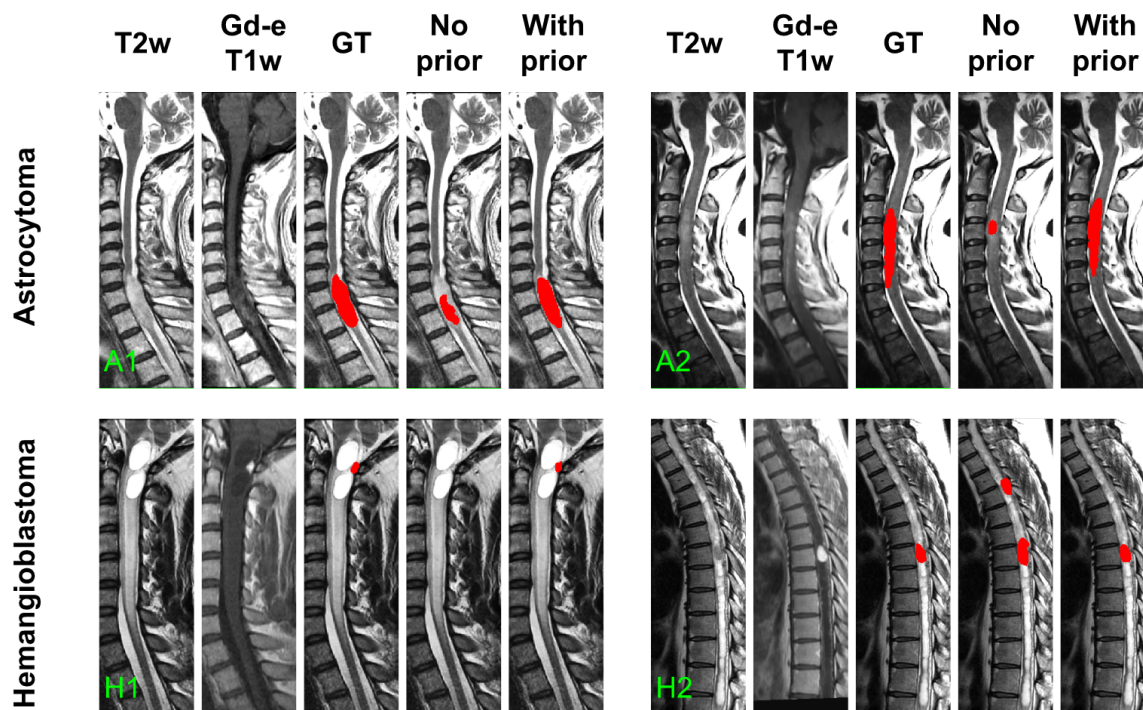


Figure 3: Tumor segmentation prediction by FiLMed U-Net informed by the tumor type, “With prior”, or not, “No prior”. A1 and A2 presents two subjects with astrocytomas. H1 and H2 presents two subjects with hemangioblastomas. GT: Ground truth.

Astrocytomas are typically large, have ill-defined boundaries, and present heterogeneous, moderate, or partial enhanced in the Gd-e T1w contrast (Baleriaux, 1999). Astrocytomas are usually extensive expanding from 2-19 vertebral bodies in size (Baleriaux, 1999). In both A1 and A2 predictions from the model without prior information, the segmented tumor size was one vertebral body or less and only segmented the most enhanced section of the tumor in Gd-e T1w.

In counterpart, hemangioblastomas are usually associated with a small tumor core (Baleriaux, 1999) intensely enhanced on Gd-e T1w (Baker et al., 2000). Figure 3 H1 presents a hemangioblastoma barely apparent in T2w and hidden by the cavity (hyperintense signal). The small hyperintense signal on the Gd-e T1w contrast was overseen by the regular approach. On H2, the model oversegmented the tumor and identified a second tumor on a hypointense signal. The false positive tumor identification does not present an intense Gd-e T1w enhancement which is usually the case for hemangioblastomas. This false positive is not present for model informed by the tumor type.